Morphological, histological and ultrastructural studies on the ovaries of *Liza carinata* from the suez bay in correlation with its reproductive cycle

Fawzia A. A. Abd El-Rahman[1], Hamza A. El-Shabaka[1], William Rizkalla[1], Azza A. El-Ganainy[2], and Mazaya E. Abo-Mosallam[1]

1- Department of Zoology, Faculty of Science, Ain Shams University, Abbassia, Cairo, Egypt.
2- National Institute of Oceanography and Fisheries, Suez branch, 183, Suez, Egypt.

ABSTRACT

Liza carinata is considered as a common and economically important Mugilidae fish of the Red Sea. Knowledge of the gonadal cycle in fishes has a great importance in the successful management of fisheries. The present study was undertaken to gain more information about the morphological, histological and ultrastructural aspects of the ovaries of *L. carinata* during the different seasons of its reproductive cycle in the Suez Bay.

The maturity stages of the ovaries of *L. carinata* can be classified into four stages, namely: the early post-spawning, late post-spawning, pre-spawning and spawning stages. Besides, *L. carinata* spawns from late September to late December. Moreover, the oogenesis of *L. carinata* is divided into seven stages. These stages are the oogonia, chromatin-nucleolar, early peri-nucleolar, late peri-nucleolar, vacuolated, early yolk globular and late yolk globular stages. In addition, the ovaries also contain the post-ovulatory structures and atretic follicles. The former are formed of the hypertrophied follicular cells after the discharge of the mature ovum, while the latter are formed as a result of the sudden cease growth of the oocytes. The present observations may help in understanding the strategy of reproduction of *L. carinata* in the Suez Bay that may help in its aquaculture.

Keywords: *Liza carinata*- ovaries- morphology- oogenesis- Zona Radiata- histology- ultrastructure.

INTRODUCTION

Sathyanesan (1961 and 1962) revealed that the ovary of *Barbus stigma* and *Mystus seenghala*, respectively, passes through four stages, namely: the growth, maturation, depletion and resting stages. In addition, Al-Daham and Bhatti (1979) found that the regular annual cycle of the ovary of *Barbus luteus* is divided into five different stages, based on various criteria as the ovarian size, colour, gonado-somatic index, average of ova diameter and histological composition, namely: the resting, preparatory, pre-spawning, spawning and post-spawning stages. Moreover, Chelemal *et al*. (2009) found that the ovary of *Liza abu* has six maturity stages, namely: the immature, resting, developing, developed, spawning (ripe) and post spawning stages.

Droller and Roth (1966) reported that the early stages of oocytes of *Lebistes reticulatus* are characterized by the presence of proliferated Golgi apparatus and rough endoplasmic reticulum. Moreover, Cárdenas *et al*. (2008) and Abdel-Aziz *et al*. (2012) stated that the ooplasm of the oocytes of *Chirostoma humboldtianum* and *Scarus ferrugineus*, respectively, at the primary growth stage, possess numerous free ribosomes, rough endoplasmic reticulum and mitochondria.

Kowtal (1967) reported that the spawning of *Mugil cephalus* in the Chilka Lake occurs from October to December. In addition, Claridge and Potter (1985) reported that *Liza ramada*, in Bristol Channel, spawns between April and June. Besides,

Chelemal *et al*. (2009) pointed out that the spawning season of *Liza abu*, in the water of Khozestan, extends from February to June. Furthermore, Albieri *et al*. (2010) stated that the spawning season of *Mugil liza* extends from May to August in the tropical bay.

Guraya *et al*. (1975) and El-Serafy *et al*. (1988) reported that, in *Mystus tengara* and *Lutjanus lineolatus*, respectively, the yolk nucleus firstly appears in the ooplasm close to the nuclear membrane of the early oocyte stage. But, as the oocyte development proceeds, the yolk nucleus migrates towards the peripheral region of the ooplasm, where it shows signs of breakdown and finally disappears. In addition, Bisht and Joshi (1975) stated that the yolk nucleus of the oocyte of *Schizothorax richardsonii* may have a relationship with the process of vitellogenesis.

Rizkalla and Yoakim (1977) distinguished hyperplasic and hypertrophic atretic follicles in the ovary of *Synodontis schall* which lead to the formation of the pre- and post-ovulatory corpora lutea, respectively.

Nassar (1993) described six stages of oocytes development of *Siganus canaliculatus*, namely: the oogonium, chromatin-nucleolar, peri-nucleolar, vacuolated, yolk globular and mature stages. In addition, Ravaglia and Maggese (2002) reported that the oogenesis of *Synbranchus marmoratus* is divided into four stages, namely: the oogonia, primary growth, cortical alveoli and vitellogenesis stages. Moreover, El-Halfawy *et al*. (2007) showed that the oocyte maturation of *Liza ramada* is divided into seven stages, namely: the chromatin-nucleolus, the early peri-nucleolus and late peri-nucleolus, the vacuolization, the yolk, the mature and the ripe stages. Besides, Cárdenas *et al*. (2008) stated that the oogenesis of *Chirostoma humboldtianum* is divided into five stages, namely: oogonium and folliculogenesis, primary growth, cortical alveoli and lipid inclusions, vitellogenesis and maturation stages. Furthermore, Uribe *et al*. (2012) reported that the oogenesis of *Crenichthys baileyi* and *Empetrichthys latos* is divided into four stages, namely: oogonia, chromatin-nucleolus, primary growth and secondary growth stages.

Assem *et al*. (2008) and Al-Absawy (2010) showed that the vacuolated oocyte wall of *Mugil cephalus* and *Merluccius merluccius*, respectively, consists of five different layers, namely: the thecal layer, follicular layer, zona radiata externa, zona radiata interna and cortical alveoli.

Kaviani *et al*. (2013) stated that the zona radiata of immature and primary growth stages of the oocytes of *Danio rerio* is not observed. However, in the peri-nucleolar and vacuolated stages of oocytes, the zona radiata is observed as a thin layer around the oocyte. Moreover, it increases in thickness at the vitellogenic stage, but reduces in maturation stage.

MATERIALS AND METHODS

The animal:

220 female specimens of *L. carinata*, ranging from 8-18.9 cm as a total length and 5-72 gm as a total body weight, were collected alive from the Suez Bay of the Red Sea which is about 120 kilometers east of Cairo.

The date of capture:

The female specimens of *L. carinata* were collected during two successive years (January 2009 to January 2011) and the capture of the specimens was performed twice per season.

The morphological studies:

The female specimens of *L. carinata* were dissected and the ovaries were dissected free, removed out, blotted by a filter paper and the length and diameter of each ovary were recorded for each specimen. Moreover, the ovaries were grossly examined and were placed in the proper stage of maturity, according to the size, shape and colour.

The histological studies:

The dissected ovaries of the female specimens of *L. carinata* were fixed immediately in freshly prepared aqueous Bouin's fluid for 24 hours. The tissues were dehydrated in ethyl alcohol, cleared in the terpineol, embedded in parablast and then were sectioned. Then the sections (6-8 μm) were stained with hematoxylin and eosin.

After staining, the sections of the ovaries were carefully examined and photomicrographs were made. Measurements were taken by using the research microscope with a measuring calibrated eye piece micrometer.

The ultrastructural studies:

Small pieces of the ovary were fixed in cold 3% glutaraldehyde solution in phosphate buffer (pH 7.4) for 2 hours at 4°C. The materials were then post-fixed in 2% osmium tetraoxide (OsO_4) for one hour in a dark place at 4°C. After that, the materials were dehydrated in an ascending ethyl alcohol series ten minutes each, at 4°C. The materials were then cleared in propylene oxide and infiltrated with and embedded in epoxy resin at 60°C.

Semithin sections (1 μm thick) were cut with the RMC-MT7 ultramicrotome and stained with toluidine blue. The semithin sections of the ovary were then examined to select the suitable areas for ultrathin sectioning.

Ultrathin sections (600 A° thick) were cut and stained with uranyl acetate and lead citrate according to Reynolds (1963). Finally, the sections were then examined with JOEL 1010 transmission electron microscope at the Regional Center for Mycology and Biotchnology, Al-Azhar University and at the National Cancer Institute, Cairo University. In addition, the grids were also examined with JOEL 1200 EXII at the Electron Microscope Unit, the Central Laboratory, Faculty of Science, Ain Shams University.

RESULTS

The morphological studies:

The ovaries of the adult female ***L. carinata*** are represented by a pair of elongated bodies which are located in the abdominal cavity and are attached to the dorsal body wall by the mesovaria. The two ovaries are separated throughout their length. The size, shape, colour and diameter of the ovaries differ according to the maturity stage of the fish during the different seasons of the year. The maturity stages of the ovaries can be classified into the following four stages, namely: the early post-spawning stage (from late December to late March), late post-spawning stage (from late March to late June), pre-spawning stage (from late June to late September) and spawning stage (from late September to late December).

The early post-spawning stage:

The ovaries are greatly reduced in size, buff or pale pink in colour and occupy about half of the length of the abdominal cavity. A few opaque residual ova are present and may be seen through the ovarian wall. The average length of the ovary is about 3.9 cm, while the average diameter is about 0.44 cm (Fig. 1A).

The late post-spawning stage:

The ovaries appear as buff or pale pink threads which occupy slightly less than half of the length of the abdominal cavity and their ova cannot be detected even with a dissecting microscope. The average length of the ovary is about 3.6 cm, while its average diameter is about 0.3 cm (Fig. 1B).

The pre- spawning stage:

The ovaries are pale yellow in colour and occupy more than half of the length of the abdominal cavity. The small ova are easily identified. The average length of the ovary is about 4.5 cm and its average diameter is about 0.55 cm (Fig. 1C).

The spawning stage:

The mature ovaries become dark yellow in colour and fill the majority of the abdominal cavity. The mature ova are large in size and are easily seen by the naked eye. The average length of the ovary is about 5.8 cm, while the average diameter is about 0.92 cm (Fig. 1D).

The histological and ultrastructural studies:

Histologically, the ovary of *L. carinata* consists of oocytes at the different maturity stages of oogenesis which are surrounded by the ovarian wall. In addition, there are degenerative oocytes (the atretic follicles) in the ovary. The ovary is divided by numerous ovigerous lamellae that projecting from the ovarian wall towards the central ovarian lumen. The developing oocytes are embedded in these ovigerous lamellae without any specific arrangement (Fig. 2).

The ovarian wall:

The ovarian wall of *L. carinata* is composed of two layers, an outer thin peritoneal layer and an inner thick tunica albuginea. The peritoneal layer is formed of simple squamous epithelial cells, while the tunica albuginea is formed of smooth muscle fibers which are arranged into two layers, an outer longitudinal muscle layer and an inner circular muscle one (Fig. 3). These two muscle layers are not completely separated, as they are sometimes intermingled with each other.

The thickness of the tunica albuginea displays seasonal variations. The thickness of the tunica albuginea during the early post-spawning season is approximately equal to 61 µm (Fig. 3), while during the late post-spawning season this layer measures about 82 µm. In addition, the thickness of the tunica albuginea of the pre-spawning season is approximately equal to 29 µm, while that of the spawning season is about 19 µm (Fig. 4).

The oogenesis:

Examination of the serial sections of the ovaries at the different seasons of the year reveals that the oocyte passes through various developmental stages to form the mature oocyte. On the bases of size variations and the nature of the nucleus, nucleolus, ooplasm and the oocyte wall, which surrounds the developing oocyte, the oogenesis in *L. carinata* is divided into seven stages. These stages are the oogonia, chromatin nucleolar, early peri-nucleolar, late peri-nucleolar, vacuolated, early yolk globular and late yolk globular stages.

The oogonia stage:

The oogonia are found as faintly stained clusters, (Fig. 5), or solitary cells adjacent to the ovigerous lamellae (Fig. 3). The oogonium is small spherical or ovoid cell with a scanty faintly stained ooplasm and a rounded or oval large nucleus which is centrally located (Figs. 3 and 5). The oogonia stage has a high nucleo-cytoplasmic ratio; the average diameter of the spherical oogonium is about 8 µm and the average diameter of the rounded nucleus is about 6 µm.

Ultrastructurally, the ooplasm of the oogonium contains few ribosomes, round mitochondria with few cristae and a poorly developed endoplasmic reticulum, while the nucleus possesses a single, spherical and centrally located nucleolus (Fig. 6).

The oogonia are usually encountered in the different seasons, but they predominate in the early and late post-spawning and pre-spawning seasons, while they are less numerous in the spawning season.

The chromatin-nucleolar stage:

The chromatin-nucleolar oocytes have a high nucleo-cytoplasmic ratio and they are polygonal or ovoid in shape with a deeply stained ooplasm (Figs. 3 and 7). The long axis of this oocyte ranges from 15.6 to 30 µm with an average of about 23.3 µm. The nucleus of this stage is large, eosinophilic and centrally located with an average diameter of about 13.6 µm. Each nucleus possesses one or two peripheral nucleoli (Fig. 7).

Ultrastructurally, the chromatin-nucleolar stage is characterized by a highly granular ooplasm due to the presence of a huge number of free ribosomes. The nucleus becomes more electron lucent than the oogonia stage and has an irregular shape with few nucleoli that migrate towards the nuclear membrane. There are numerous and elongated mitochondria with few cristae. This stage is surrounded by the prefollicular cells which are flattened in shape with long and thin processes that surround the oocyte. The nuclei of the prefollicular cells are flattened with chromatin patches (Fig. 8). The relation between the cell membranes of the prefollicular cells and the oolemma of this oocyte stage is smooth and they run parallel to each other with a narrow intercellular space (Fig. 9).

This stage is usually encountered in the different seasons of the year. They predominate in the early and late post-spawning and pre-spawning seasons, but they are less numerous in the spawning season.

The early peri-nucleolar stage:

The early peri-nucleolar oocyte is more or less spherical in shape with a diameter ranging from 27 µm to 75 µm; the average diameter is about 51 µm. The nucleus is rounded in shape and appears eosinophilic or faintly stained with an average diameter of about 40 µm. The nucleus possesses numerous peripheral nucleoli. Occasionally, one of these nucleoli appears larger in size than the remaining ones and some of these nucleoli are seen inside vacuoles (Fig. 5). The ooplasm is deeply stained and appears as a homogeneous and finely granulated mass. The yolk nucleus or nuages or Balbiani's body appears as a cap of deeply stained substance at one side of the nucleus (Fig. 10).

Ultrastructurally, this stage is characterized by a highly granular ooplasm due to the abundance of free ribosomes (Fig. 11). The nucleus of this stage is electron lucent and spherical with numerous peripheral nucleoli that situated near the nuclear membrane. The nuclear membrane exhibits numerous nuclear pores through which an electron dense, granular material migrates from the nucleus to the ooplasm and frequently appears associated with the mitochondria (Fig. 12). Moreover, the Golgi apparatus is found near the cell periphery (Fig. 11).

Histologically, this stage is enveloped with an oocyte wall which is formed of two layers, namely: the follicular layer and the thecal one (Fig. 13). Ultrastrurally, there is also a distinct basal lamina which is a noncellular layer separating the follicular layer from the overlying thecal layer. Both the follicular and thecal cells are flattened and elongated cells. The nuclei of these cells are elongated, irregular in shape and have dense chromatin patches, while their cytoplasm has free ribosomes and endoplasmic reticulum (Fig. 14).

The first sign of the morphological specialization of the oolemma is the formation of the microvilli. The surface of this oocyte is completely covered with the long microvilli which project into the intercellular space between the oocyte and the follicular cells. This space is produced when the follicular cells move away from the surface of the oocyte during the early growth period (Fig. 15).

The early peri-nucleolar oocytes are usually encountered in all the seasons of the year. However, they increase in number during the early and late post-spawning and the pre-spawning seasons, while they are fewer in number during the spawning season.

The late peri-nucleolar stage:

The late peri-nucleolar oocyte appears mostly spherical in shape with a diameter ranging from 65 µm to 105 µm; the mean diameter is about 85 µm. Each oocyte contains a large spherical, eosinophilic and centrally located nucleus that has a mean diameter of about 50 µm. The nucleus contains a large number of nucleoli which are arranged at the periphery near the nuclear membrane (Fig. 16). The ooplasm is a homogenous finely granulated material and its basophilia is less than that of the early peri-nucleolar stage (Fig. 17).

In this stage, the yolk nucleus becomes a small basophilic body which lies in the peripheral ooplasm (Fig. 17) and then completely disappears.

Ultrastructurally, the late peri-nucleolar stage is similar to the early peri-nuclear one, but it becomes larger and has a less electron dense ooplasm than the previous stage (Fig. 15). The nucleus of this stage is electron lucent and has numerous peripheral nucleoli. The yolk nucleus is found in the ooplasm and is formed of a spherical homogenous mass (Fig. 18), then it is compeletly dispersed and is no longer seen in the ooplasm. The ooplasm contains numerous free ribosomes, mitochondria and endoplasmic reticulum (Fig. 19).

Histologically, the oocyte wall of this stage possesses a very thin and hardly detectable zona radiata, external to which the follicular layer lies. The latter is in turn surrounded by the thecal layer (Fig. 20). Ultrastructurally, the oocyte wall consists of four layers, namely: the zona radiata, follicular layer, basal lamina and thecal layer. During this stage, the zona radiata begins to be deposited as a homogeneous, electron dense material which its thickness is about 0.29 µm. There are finger-like microvilli traversing the zona radiata through the pore canals. Both the follicular and thecal cells are of the simple squamous type with flattened nuclei and few cytoplasmic organelles which are represented mostly by some short profiles of endoplasmic reticulum, mitochondria and ribosomes (Fig. 19).

The late peri-nucleolar oocyte stage is found in the different seasons of the year. They predominate in the pre-spawning season, but they are less numerous in the early and late post-spawning seasons and they are very few during the spawning season.

The vacuolated stage:

The vacuolated oocytes are more or less oval in shape and are characterized by the presence of transparent and spherical vacuoles which are variable in size and scattered in the ooplasm (Fig. 21).

Each vacuolated oocyte increases in size with a long axis ranging from 100 µm to 166 µm and the average is about 139 µm. The nucleus is rounded or oval in shape (Fig. 21). The average long axis of the oval nucleus is about 68 µm. The nuclear membrane is wavy forming several outpocketings, in which the peripheral nucleoli are located (Fig. 22).

Ultrastructurally, the vacuolated stage is characterized by the lipid synthesis, leading to an increase in lipid stores. The lipid droplets are homogeneous and are

accumulated first around the nucleus (Fig. 23). Moreover, they eventually become distributed randomly in the ooplasm (Fig. 24). Each lipid droplet has an electron dense core and an outer electron lucent zone. The nucleus of this stage of oocyte has an irregular nuclear membrane and numerous peripheral nucleoli (Fig. 23). Between the lipid droplets, there are numerous mitochondria and many vacuoles that have electron lucent and finely granular contents (Fig. 24).

Histologically, the zona radiata becomes more obvious and is surrounded externally by a follicular layer beneath the outermost thecal layer (Fig. 25). Ultrastructurally, the oocyte wall consists of four layers, namely: the zona radiata, follicular layer, basal lamina and thecal layer. During this stage of development, the zona radiata is relatively thicker than that of the previous stage and its thickness is about 1.6 µm and has few rows of pore canals (Fig. 26). Both the follicular, (Fig. 26), and thecal, (Fig.27), cells have the same structures as those of the previous stage.

The vacuolated oocytes are mainly observed during the spawning season, but they are less numerous in the pre-spawning season and they are absent in the early and late post-spawning seasons.

The early yolk globular stage:

The early yolk globular oocytes are more or less rounded in shape and are characterized by substantial growth which is primarily accounted for the accumulation of yolk granules into the ooplasm. The diameter of this oocyte ranges from 170 µm to 230 µm with an average diameter of about 200 µm. The ooplasm of this oocyte is characterized by the deposition of the eosinophilic yolk granules which are accumulated very rapidly (Figs. 28 and 29). There are also numerous vacuoles which are distributed between the yolk granules (Figs. 29 and 30).

At the beginning of this stage, the nucleus is still eosiophilic in nature and ovoid in shape with numerous peripheral nucleoli (Fig. 28). The nucleus has an average long axis of about 67 µm. With the oocyte growth, the nucleus becomes deeply stained, irregular in shape and slightly decreases in size with an average long axis of about 50 µm (Fig. 29).

Ultrastructurally, the ooplasm of early yolk globular oocyte is filled with rounded yolk granules (Fig. 31), which are accumulated from the outside into the ooplasm through the pore canals of the zona radiata (Fig. 32). In addition, there are numerous large lipid droplets and vacuoles that are alternating with the yolk granules in the ooplasm (Fig. 31).

Histologically, the oocyte wall of this stage has the same structure as that of the vacuolated stage, but the zona radiata becomes thicker and is still surrounded externally by the follicular and thecal layers (Fig. 30). Ultrastructurally, the oocyte wall consists of four layers, namely: the zona radiata, follicular layer, basal lamina and thecal layer. Concomitant with the growth of the oocyte, the zona radiata has a mean thickness about 6.8 µm and is differentiated into the inner thick zona radiata interna and the outer thin zona radiata externa. During this stage of development, the zona radiata interna has numerous rows of pore canals, while the zona radiata externa has only a single row of pore canals. The abundant finger-like microvilli are embedded in the zona radiata and traverse it through the pore canals to reach the follicular cells. Both the follicular and thecal cells have the same structures as those of the previous stage and do not show any marked changes throughout the oocyte development (Fig. 33).

The early yolk globular oocytes are observed during the spawning season only.

The late yolk globular stage:

The late yolk globular oocyte is large in size, mostly spherical in shape (Fig. 34). The diameter of this oocyte stage ranges from 223 µm to 415 µm with an average diameter of about 319 µm. The yolk granules of these oocytes tend to coalesce to form globules. In addition, the vacuoles also coalesce together to form many larger vacuoles (Fig. 35). The nucleus of this oocyte stage is irregular, deeply stained and starts to migrate to the oocyte periphery (Fig. 35), then it becomes completely invisible (Fig. 34).

Histologically, the oocyte wall is well developed and consists of the zona radiata, follicular layer and thecal layer (Fig. 36). Ultrastructurally, the oocyte wall becomes very thick and consists of four layers, namely: the zona radiata, follicular layer, basal lamina and thecal layer (Fig. 37). Concomitant with the oocyte growth, the zona radiata exhibits distinct striations with reticulate pattern. It increases in thickness which is about 24 µm and is transversed perpendicularly by the pore canals. The zona radiata interna is thick and possesses numerous rows of the pore canals, while the zona radiata externa maintains a compact homogenous structure with few rows of the pore canals (Figs. 37 and 38). Prior to ovulation, the follicular and thecal cells show degeneration and become relatively small with elongated oval heterochromatic nuclei (Fig. 38).

The late yolk globular oocytes are observed during the spawning season only.

The post-ovulatory structure:

After the ovum is discharged from the mature follicle, the latter undergoes remarkable structural variations which lead to the formation of the post-ovulatory structure that disappears rapidly in the ovarian stroma. The post-ovulatory structure is seen as a collapsed mass of epithelial cells. The follicular cells of the post-ovulatory structure hypertrophy and make folds into the oocyte lumen which has been previously occupied by the ovum. The hypertrophied follicular cells are cuboidal or short columnar in shape with an eosinophilic cytoplasm and rounded basophilic nuclei (Fig. 39).

The post-ovulatory structures have a very short life span, since they are only encountered during the early post-spawning season.

The atretic follicles:

During the course of oogenesis, some follicles may suddenly cease growth and become atretic. The early signs of atresia are shown by the disappearance of the nucleus and the breakdown of the zona radiata and its subsequent disappearance. In addition, the simple follicular layer becomes stratified and the follicular cells become cuboidal in shape and invade the underlying liquefied yolk (Figs. 40 and 41). As the process of atresia proceeds, the liquefied yolk becomes scare, loose and intermixed with the invading follicular cells. In addition, the zona radiata becomes very thin and shows highly breakdown (Fig. 42). Finally, the atretic follicles are resorbed through the ovarian stroma.

The atretic follicles are mainly observed during the late post-spawning season, but they are very few during the early post-spawning, pre-spawning and spawning seasons.

DISCUSSION

Depending on the variations of the size, shape and colour of the ovaries, the maturity stages of the ovaries of *L. carinata* can be classified into four stages, namely: the early post-spawning, late post-spawning, pre-spawning and spawning stages.

Similarly, Barbieri *et al*. (1981) distinguished four stages in the ovary of *Geophagus brasiliensis*, namely: the immature, maturing, mature and spent stages. On the other hand, El-Agamy *et al*. (1987) classified the ovaries of *Lethrinus lentjan* morphologically into six stages, namely: dormancy, intermediate, maturing, mature, ripe and post-spawning stages. Besides, Al-Absawy (2010) stated that the general pattern of developmental stages of the ovaries of *Merluccius merluccius* is classified into six stages, namely: immature, maturing, nearly ripe, ripe, spawning and spent stages. Moreover, Mercy *et al*. (2013) reported that the maturity stages of the ovaries of *Puntius denisonii* are classified into five stages, namely: the immature, maturing, ripening, ripe and spent stages.

In fisheries studies, the spawning season is an important factor for regulating fisheries (King, 2007). In the present study, the spawning season of *L. carinata,* from the Suez Bay, extends from late September to late December. Similarly, Salem and Mohammed (1982) showed that the spawning season of *Mugil seheli* in Lake Timsah occurs in December. Moreover, El-Boray (1993) pointed out that the spawning season of *Mugil seheli* in Suez Bay extends from November to March. Besides, Ismail *et al.* (1998) pointed out the natural spawning season of *L. carinata,* from Sulaibikhat Bay occurred between December and February. Moreover, Mahmoud (1997) indicated that the spawning season of *Mugil seheli*, reared in farms, is sharp in November and December, while, El-Halfawy (2004) showed that the spawning season of *Mugil seheli,* reared in fish farms, is August and September.

The ovarian wall of *L. carinata* is composed of two layers, an outer thin peritoneal layer and an inner thick tunica albuginea. The latter is formed of smooth muscle fibers which are arranged into two layers, an outer longitudinal layer and an inner circular one. Moreover, the presence of smooth muscle fibers in the tunica albuginea of *L. carinata* may play an important role in the discharge of the ova to the exterior. These results are in accordance with those described in *Schilbe mystus* (El-Dawi, 1990) and in *Siganus canaliculatus* (Nassar, 1993). On the other hand, Lehri (1968) and Boulos and Ashour (1973) stated that the tunica albuginea of *Clarias batrachus* and *Solea vulgaris*, respectively, is formed mainly of connective tissue layer, containing some patches of smooth muscle fibers.

The thickness of the tunica albuginea of *L. carinata* displays seasonal variations. During the early and late post-spawning seasons, the tunica albuginea is thick and becomes thin in the pre-spawning season and very thinner in the spawning season. These observations are in accordance with those of Emam and Abughrien (2014) in *Clarias lazera*, who also stated that the thin tunica albuginea of the ovary in spawning season is due to pressure exerted on it by the enlarged mature oocytes.

The oogenesis in *L. carinata* is divided into seven stages, namely: the oogonia, chromatin nucleolar, early peri-nucleolar, late peri-nucleolar, vacuolated, early yolk globular and late yolk globular stages. These results are in agreement with those of Coward and Bromage (1998), in *Tilapia zillii*, and El-Boray and El-Gharabawy (1999), in *Gerres oyena*.

The oogonia of *L. carinata* are found as faintly stained clusters or solitary cells adjacent to the ovigerous lamellae. Each oogonium is spherical or ovoid in shape with a rounded and centrally located nucleus. These observations coincide with those of *Thunnus obesus* (Figueiredo *et al.,* 2008) and of *Barbus luteus* and *Varicorhinus trutta* (Rahemo and Al-Shatter, 2012). In addition, the ultrastructural studies revealed that the oogonia of *L. carinata* possess a scanty amount of ooplasm with few ribosomes, rounded mitochondria with few cristae and poorly developed endoplasmic

reticulum. Similar results were reported by Assem *et al.* (2008) in *Mugil cephalus*, and Al-Absawy (2010) in *Merluccius merluccius*.

The chromatin-nucleolar oocyte of *L. carinata* appears as a small polygonal or ovoid cell with a slightly deeply stained ooplasm and large eosinophilic nucleus. These results are similar to those described by Zaki and El- Gharabawy (1991) in *Mugil capito* and Al-Absawy (2010) in *Merluccius merluccius*. Moreover, the ultrastructural studies postulated that the ooplasm of the chromatin-nucleolar oocyte of *L. carinata* is highly granular and is provided by a huge number of free ribosomes. In addition, the nucleus becomes more electron lucent than that of the oogonium and it has an irregular shape with few nucleoli that migrate towards the nuclear membrane. These observations are in agreement with those found by Gaber (2000) in *Bagrus bayad*.

The chromatin-nucleolar oocyte of *L. carinata* is surrounded by the prefollicular cells which are flattened and with long and thin processes. The relation between the cell membrane of the prefollicular cells and the oolemma of the oocyte is smooth and they run parallel to each other with a narrow intercellular space. Similar results were found in *Syngnathus scovelli* (Begovac and Wallace, 1988) and in *Crenichthys baileyi* (Uribe *et al.,* 2012).

The early peri-nucleolar oocytes of *L. carinata* are more or less spherical in shape and have eosinophilic nuclei with numerous peripheral nucleoli. These observations are in agreement with those of Nassar (1993) in *Siganus canaliculatus* and Assem (2003) in *Pagellus erythrinus,* who stated that the increase in the number of nucleoli of the peri-nucleolar oocytes of the teleosts is due to the fragmentation of the original nucleolus.

The early peri-nucleolar oocyte of *L. carinata* is characterized by the presence of the yolk nucleus which starts as a cap of deeply stained substance near the nucleus and then, in the late peri-nucleolar oocyte, it becomes a small basophilic body that moves towards the peripheral ooplasm. Similar observations have been noticed by Guraya *et al*. (1975), El-Serafy *et al.* (1988) and Al-Absawy (2010) in *Mystus tengara, Lutjanus lineolatus* and *Merluccius merluccius*, respectively. Moreover, Nayyar (1964) suggested that the yolk nucleus may initiate the synthesis of lipids. On the other hand, Beams and Kessel (1973) suggested that the yolk nucleus of *Salmo gairdneri* constitutes an essential precursor substance, perhaps RNA, necessary for the oocyte growth and yolk formation. Furthermore, these yolk nuclei are found at the beginning of the oocyte development of *L. carinata* and disappear at the end of the late peri-nucleolar oocyte stage. This finding is in accordance with that recorded by Cárdenas *et al.* (2008) in *Chirostoma humboldtianum*, but contradicts with that of Abascal and Medina (2005), who stated that the yolk nuclei in *Thunnus thynnus* persist until the lipid stage.

Furthermore, the ultrastructural study revealed that the early peri-nucleolar stage of *L. carinata* is characterized by the presence of the granular materials opposed to the nuclear membrane at the ooplasmic side. This result is similar to that of Abascal and Medina (2005), Cárdenas *et al.* (2008) and Uribe *et al.* (2012) in *Thunnus thynnus, Chirostoma humboldtianum* and *Empetrichthys latos,* respectively. In addition, the electron dense and granular nuclear materials of the late peri-nucleolar stage of *L. carinata* are migrated from the nucleus to the peripheral ooplasm forming, with the mitochondria, the yolk nucleus. These observations are in accordance with those reported by Grier (2000), Abascal and Medina (2005) and Mazzoni *et al.* (2010) in *Centropomus undecimalis*, *Thunnus thynnus* and *Cyprinus carpio,* respectively.

The present results showed that the vacuolated stage of *L. carinata* is characterized by the lipid synthesis, leading to an increase in lipid stores. Each lipid droplet has an electron dense core and an outer electron lucent zone. Similar observations have been noticed in *Thunnus thynnus* (Mourente *et al.*, 2002), in *Synbranchus marmoratus* (Ravaglia and Maggese, 2002) and in *Chirostoma humboldtianum* (Cárdenas *et al.* 2008). In *L. carinata*, there are many vacuoles, between the lipid droplets, that have electron lucent and finely granular contents. The same observation was recorded in *Caranx crysos* and *Pagellus erythrinus* (Assem, 2000 and 2003, respectively) and in *Merluccius merluccius* (Al-Absawy, 2010).

The present results showed that the early and late yolk globular oocytes of *L. carinata* are characterized by the deposition of the eosinophilic yolk granules in the ooplasm which are accumulated very rapidly and coalesce to form masses or globules. In addition, the ooplasm possesses numerous lipid droplets and vacuoles which also coalesce together to form many larger ones. Similar observations were reported by many authors, such as Assem (2000) in *Caranx crysos,* Dadzie *et al.* (2000) in *Pampus argenteus*, Assem (2003) *Pagellus erythrinus* and Chen and Tzeng (2009) in *Chaetodontoplus septentrionalis.* In addition, the nucleus of the late yolk globular oocyte of *L. carinata* is irregular deeply stained and starts to migrate to the oocyte periphery then it becomes completely invisible. Similar results were reported by Chen and Tzeng (2009) in *Chaetodontoplus septentrionalis.*

The early peri-nucleolar oocyte of *L. carinata* is enveloped with an oocyte wall which is formed of two layers, namely: the follicular layer and the thecal one. Both follicular and thecal layers are formed of flattened cells with flattened nuclei. These results are in accordance with those described in *Synbranchus marmoratus* (Ravaglia and Maggese, 2002). In addition, the wall of the late peri-nucleolar oocyte of *L. carinata* has a very thin and hardly detectable zona radiata, external to which the follicular layer lies. The latter is in turn coated by the thecal layer. Similar observations were noticed in *Pseudotylosurus microps* (Cruz-Landim and Cruz-Hofling, 2001), in *Mugil cephalus* (Assem *et al.*, 2008) and in *Chirostoma humboldtianum* (Cárdenas *et al.,* 2008).

The first sign of the morphological specialization of the oolemma of the early peri-nucleolar oocyte stage of *L. carinata* is the formation of the microvilli which cover the surface of the oocyte and project into the intercellular space. These observations coincide with those obtained by Cárdenas *et al.* (2008) in *Chirostoma humboldtianum.*

In *L. carinata,* the ultrastructural study showed that the oocyte wall, from the late peri-nucleolar stage to the end of the oocyte maturation stage, consists of four layers, namely: the zona radiata, follicular layer, basal lamina and thecal layer. Furthermore, the zona radiata of the yolk globular oocyte of *L. carinata* is differentiated into an inner thick zona radiata interna and an outer thin zona radiata externa. A similar result was reported by Al-Absawy (2010) in *Merluccius merluccius.*

During the oocyte maturation of *L. carinata*, the zona radiata begins to be deposited as a homogeneous, moderately electron dense material. This result agrees with that of Abascal and Medina (2005) and Cárdenas *et al.* (2008) in *Thunnus thynnus* and *Chirostoma humboldtianum,* respectively. Moreover, the thickness of the zona radiata increases concomitantly with the oocyte maturation and it possesses numerous rows of pore canals. The same observations were recorded in *Gerres oyena* (El-Boray and El-Gharabawy, 1999), in *Chirostoma humboldtianum* (Cárdenas *et al.,* 2008) and in *Merluccius merluccius* (Al-Absawy, 2010). In addition, these results

contradict with those of El-Serafy *et al.* (1988) who stated that the zona radiata of *Lutjanus lineolatus* is hardly detectable even in the mature follicles.

In *L. carinata*, the microvilli of the oocyte traverse the thickened zona radiata through the pore canals to reach the follicular cells. These observations coincide with those obtained by Selman and Wallace (1983) in *Fundulus heteroclitus*, Assem (2003) in *Pagellus erythrinus* and Cárdenas *et al.* (2008) in *Chirostoma humboldtianum*. The zona radiata of *L. carinata* may be used in the nutritive material transfer from the follicular cells to the oocytes through the pore canals. This function was also proposed by Hurley and Fisher (1969) in *Salvelinus fontinalis* and El-Boray and El-Gharabawy (1999) in *Gerres oyena*. In addition, Dadzie (1968) stated that the zona radiata of *Tilapia mossambica* plays an important role in the protection of the oocyte from the substratum; the zona radiata swells and becomes firm when it mixed with the ambient water.

In *L. carinata*, the zona radiata may be produced by the follicular cells. A similar conclusion was arrived at by Rizkalla (1970) in *Clarias lazera* and Kamel and Yoakim (1977) in *Synodontis schall*. On the other hand, Braekevelt and McMillan (1967) and El-Dawi (1990) stated that the zona radiata of *Eucalia inconstans* and *Schilbe mystus*, respectively, appears to be formed firstly from the ooplasm itself, since the follicular epithelium in the early stages of the egg development is poorly developed, but later on, both the ooplasm and the well developed follicular cells share in the formation of a thick zona radiata. Besides, Yamamoto (1963) and Hurley and Fisher (1969) stated that the synthesis of the zona radiata of *Oryzias latipes* and *Salvelinus fontinalis*, respectively, has been attributed to the activity of the ooplasm.

In *L. carinata,* the follicular layer of the mature oocyte consists of a single row of flattened cells. This observation contradicts with that of El-Dawi (1990) in *Schilbe mystus,* who stated that the follicular layer of the mature oocyte is formed of a stratified epithelium. Moreover, in *Mystus seenghala* (Sathyanesan, 1962) and in *Dorosoma petenense* (Shelton, 1964), the follicular epithelium of the mature oocyte is formed of a simple columnar cells. In addition, in *Chrysichthys auratus* (Shakhsheir, 1970) and in *Synodontis schall* (Kamel and Yoakim, 1977), the follicular layer of the oocyte consists of simple cuboidal cells.

The pre-vitellogenic oocytes of *L. carinata*, from the oogonia to the late peri-nucleolar oocytes, are usually encountered in the different seasons, but they predominate in the early and late post-spawning and pre-spawning seasons, while they are less numerous in the spawning season. In addition, the vitellogenic oocytes predominate mainly in the spawning season. These observations are in agreement with those found in *Schilbe mystus* (El-Dawi, 1990) and in *Clarias lazera* (Emam and Abughrien, 2014).

After the discharge of the ovum from the mature follicle, the post-ovulatory structure of *L. carinata* is formed. The follicular layer of the post-ovultory structure hypertrophies and makes folds into the oocyte lumen which has been previously occupied by the ovum. This collapsed nature may be due to the contraction of the mature follicle to achieve ovulation. Similar observations were noticed by Ravaglia and Maggese (2002) in *Synbranchus marmoratus* and Chen and Tzeng (2009) in *Chaetodontoplus septentrionalis.*

The hypertrophied follicular cells of the post-ovulatory structure of *L. carinata* are cuboidal or short columnar cells with an eosinophilic cytoplasm and oval basophilic nuclei. The post-ovulatory structures have a very short life span, since they are only encountered during the early post-spawning season. These results are in

accordance with those of Abou-Seedo *et al.* (2003) in *Acanthopagrus latus* and Üçüncü and Çakici (2009) in *Danio rerio.*

During the oogenesis of *L. carinata*, some follicles may suddenly cease growth and form the atretic follicles. The formation of these atretic follicles is usually followed by their degenerative and resorptive processes. This feature was also reported in different teleost fishes by many authors such as Chubb and Potter (1984) in *Nematalosa vlaminghi*, Ramadan *et al.* (1987) in *Sparus aurata* and Kamel (1990) in *Oreochromis niloticus*.

The atretic follicles of *L. carinata* are characterized by the breakdown of the zona radiata. As the process proceeds, the follicular cells increase in number and invade the underlying liquefied yolk. In a more advanced stage of atresia, the yolk mass becomes loose, scarce and intermixed with the invading follicular cells. These results agree with those of Abou-Seedo *et al.* (2003) in *Acanthopagrus latus* and Üçüncü and Çakici (2009) in *Danio rerio.*

The atretic follicles of *L. carinata* are usually encountered mainly in the late post-spawning season, but they are fewer in number in the other seasons. This observation agrees with that of Rizkalla and Yoakim (1977) in *Synodontis schall* and Merson *et al.* (2000) in *Paralichthys dentatus.*

REFERENCES

Abascal, F. J. and Medina, A. (2005). Ultrastructure of oogenesis in the bluefin tuna, *Thunnus thynnus.* J. Morphol., 264(2):149-160.

Abdel-Aziz, S. H.; Al-Otaibi, M.; Osman, A.M.; Ali, T. E. and Bawazeer, F. (2012). Ultrastructural evidence of oogenesis of the rusty parrotfish, *Scarus ferrugineus* (Teleostei: Scaridae) Copeia, 2: 229-236.

Abou-Seedo, F. S.; Dadzie, S. and Al-Kanaan, K. A. (2003). Histology of ovarian development and maturity stages in the yellowfin seabream *Acanthopagrus latus* (Teleostei: Sparidae) (Hottuyn, 1782). J. Appl. Ichthyol., 19: 65-73.

Al-Absawy, M. A. (2010). The reproductive biology and the histological and ultrastructural characteristics in ovaries of the female gadidae fish, *Merluccius merluccius,* from the Egyptian Mediterranean water. Afr. Biotechnol., 9 (17): 2544-2559.

Albieri, R. J.; Araujo, F. G. and Uehara, W. (2010). Differences in reproductive strategies between two co-occurring mullets, *Mugil curema* Valenciennes 1836 and *Mugil liza* Valenciennes 1836 (Mugilidae) in a tropical bay. Trop. Zool., 23(1): 51-62.

Al-Daham, N. K. and Bhatti, M. N. (1979). Annual changes in the ovarian activity of the fresh-water teleost, *Barbus luteus* (Heckel) from southren Iraq. J. Fish Biol., 14: 381-387.

Assem, S. S. (2000). The reproductive biology and histological characteristics of pelagic carangid female *Caranx crysos* from the Egyptian Mediterranean Sea. J. Egypt. Ger. Soc. Zool., (31C):195-215.

Assem, S. S. (2003). The reproductive biology and the histological and ultrastructural characteristics of the ovary of the female pelagic fish *Pagellus erythrinus* from the Egyptian Mediterranean water. J. Egypt. Ger. Soc. Zool., 42: 77-103.

Assem, S. S.; El-Dahhar, A. A. and Mourad, M. M. (2008). Reproductive biology (histological & ultrastructure) and biochemical studies in ovaries of *Mugil cephalus* from Mediterranean water. J. Arab. Aquat. Soc., 3(1): 33-58.

Barbieri, M. C.; Barbieri, G. and Marins, M. D. (1981). Anatomy and histology of the ovary of *Geophagus brasiliensis* at Lobodam State of Seo-Paulo, Brazil. Rev. Braz. Biol., 41: 163-168.

Beams, H. W. and Kessel, R. G. (1973). Oocyte structure and early vitellogenesis in the trout, *Salmo gairdneri.* Am. J. Anat., 136(1): 105-121.

Begovac, P. C. and Wallace, R. A. (1988). Stages of oocyte development in the pipefish, *Syngnathus scovelli.* J. Morphol., 197(3): 353-369.

Bisht, J. S. and Joshi, M. L. (1975). Seasonal histological changes in the ovary of a mountain stream teleost, *Schizothorax richardsonii* (Gray and Hard). Acta. Anat., 93: 612-625.

Boulos, R. and Ashour, M. B. (1973). Studies on the female reproductive cycle of some fishes at Lake Qarun (Faiyum, Egypt). IV. Seasonal morphological and macroscopical changes of the ovary of *Solea vulgaris.* Bull. Fac. Sci., Cairo Univ., 46: 235-250.

Braekevelt, C. R. and McMillan, D. B. (1967). Cyclical changes in the ovary of the brook stickleback, *Eucalia inconstans.* J. Morphol., 123: 373-396.

Cárdenas, R.; Chávez, M.; González, J. L.; Aley, P.; Espinosa, J. and Jiménez-García, L. F. (2008). Oocyte structure and ultrastructure in the Mexican silverside fish, *Chirostoma humboldtianum* (Atheriniformes: Atherinopsidae). Rev. Biol. Trop., 56(4): 1825 – 1835.

Chelemal, M.; Jamili, S. and Sharifpour, I. (2009). Reproductive biology and histological studies in Abu mullet, *Liza abu* in the water of the Khozestan Province. J. Fish. Aquat. Sci., 4 (1): 1-11.

Chen, K. Y. and Tzeng, W. N. (2009). Reproductive mode of the blue-striped angelfish, *Chaetodontoplus septentrionalis* in northeastern Taiwan. J. Zool. Stud., 48(4): 468-476.

Chubb, C. F. and Potter, I. C. (1984). The reproductive biology and estuarine movements of the gizzard shad, *Nematalosa vlaminghi* (Munro). J. Fish Biol., 25: 527-543.

Claridge, P. N. and Potter, I. C. (1985). Distribution, abundance and size composition of mullet populations in the Severn Estuary and Bristol Channel. J. Mar. Biol., Assoc. U.K., 65(2): 325-335.

Coward, K. and Bromage, N. R. (1998). Histological classification of oocyte growth and the dynamics of ovarian recrudescence in *Tilapia zillii.* J. Fish Biol., 53(2): 285-302.

Cruz-Landim, C. and Cruz-Hofling, M. A. (2001). Ultastructure of ovarian follicular epithelium of the amazonian fish *Pseudotylosurus microps* (Teleostel: Belonidae): Morphological and histological characterization of the intercellular deposits. Rev. Brasil. Biol., 61(1): 133-140.

Dadzie, S. (1968). The structure of the chorion of the egg of the mouthbrooding cichlid fish, *Tilapia mossambica.* J. Zool. Lond., 154: 161-163.

Dadzie, S.; Abou-seedo, F. and AL-Shallal, T. (2000). Reproductive biology of the silver pomfret, *Pampus argenteus* (Euphrasen), in Kuwait waters. J. Appl. Ichthyol., 16: 247-253.

Droller, M. J. and Roth, T. F. (1966). An electron microscope study of yolk formation during oogenesis in *Lebistes reticulatus* guppyi. J. Cell Biol., 28: 209-232.

El-Agamy, A. E.; El Shabaka, H. A. and Mohallal, M. E. (1987). Ovarian cycle and spawning season of *Lethrinus lentjan* Lecepede in Qatari waters, Arabian Gulf. Bull. Fac. Sci., Zagazig Univ., 9: 672- 692.

El-Boray, K. F. (1993). Reproductive biology and physiology characters of *Mugil seheli*. M. Sc. thesis, Facu. Sci. Tanta Univ., Egypt.

El-Boray, K. F. and El-Gharabawy, M. M. (1999). Histological characters of ovarian changes of *Gerres oyena* during the reproductive cycle, Suez Bay. Egypt. J. Aquat. Biol. Fish., 3 (2): 115-129.

El-Dawi, F. (1990). Studies on the hypothalamo-hypophysial complex in correlation with the ovarian cycle of a certain teleost. Ph.D. thesis, Facu. Sci. Ain Shams Univ., Egypt.

El-Halfawy, M. M. (2004). Reproductive biology of *Mugil seheli* (Family: Muglidae) reared in fish farm. Egypt. J. Aquat. Res., 30(B): 234-240.

El-Halfawy, M. M.; Ramadan, A. M. and Mahmoud, W. F. (2007). Reproductive biology and histological studies of the grey mullet, *Liza ramada*, (Risso, 1826) in Lake Timsah, Suez canal. Egypt. J. Aquat. Res., 33 (1): 434-454.

El-Serafy, S.S.; Al-Zahaby, A. S. and El-Darawany, M. A. (1988). Histological studies on the gonads of *Lutjanus lineolatus* (Bloch.) during its reproductive cycle. Inst. Oceanog. Fish. A. R. E., 14: 1-15.

Emam, M. E. and Abughrien, B. (2014). Seasonal histological changes in gonads of the catfish (*Clarias lazera*). Fish. Aquac. J., 5(1). doi: 10.4172/2150-3508.1000087.

Figueiredo, M. B.; Santos, A. G.; Travassos, C. M. and Magalhaes, B. R. (2008). Oocyte organization and ovary maturation of the bigeye tuna (*Thunnus obesus*) in the west tropical Atlantic Ocean. J. Collect., 62(2): 579-585.

Gaber, S. A. O. (2000). Biological, histological and histochemical studies on the reproductive organs and pituitary gland of *Bagrus docmac* and *Bagrus bayad* in the Nile water, with special reference to the ultrastructure of supporting tissues. Ph. D. thesis, Faculty of Science, Zagazig Univ., Egypt.

Grier, H. J. (2000). Ovarian germinal epithelium and folliculogenesis in the common snook, *Centropomus undecimalis* (Teleostei: Centropomidae). J. Morphol., 243(3): 265-281.

Guraya, S. S.; Kaur, R. and Saxena, P. K. (1975). Morphology of ovarian changes during the reproductive cycle of the fish, *Mystus tengara* (Ham.). Acta Anat., 91 : 222 – 260.

Hurley, D. A. and Fisher, K. C. (1969). The structure and development of the external membrane in young eggs of the brook trout, *Salvelinus fontinalis* (Mitchill). J. Zool., 44(2): 173-190.

Ismail, W. A.; Al-Abdul-Elah, K. and Al-Yamani, F. (1998). Larval development of the back keeled mullet, *Liza carinata*. Hydrobiol., 385(1): 87–105.

Kamel, S. A. (1990). Study of atresia in the ovary of the Nile bolti, *Oreochromis niloticus*, during its annual reproductive cycle. Proc. Zool. Soc., A. R. E., 18: 1-10.

Kamel, A. and Yoakim, E. G. (1977). Studies on the ovary of the Nile catfish, *Synodontis schall* (Bloch-Schneider). I. Histology. Proc. Zool. Soc., A. R. E., 6: 181-188.

Kaviani, E. F.; Shabanipour, N. and Mirnategh, S. B. (2013). Light and electron microscope structural study of the zona radiata in the oocyte of zebrafish (*Danio rerio*). Micros., 62(3): 377-82.

King, M. (2007). Fisheries biology, Assessment and Management. 2nd edition. Blackwell Publisher, Oxford.

Kowtal, G. V. (1967). Occurrence and distribution of pelagic fish eggs and larvae in the Chilka Lake during the years 1964 and 1965. Ind. J. Fish., 14 (1 & 2): 198-214.

Lehri, G. K. (1968). Cyclical changes in the ovary of the catfish *Clarias batrachus* L. Acta Anat., 69: 105- 124.

Mahmoud, W. F. (1997). Reproductive and physiological characters of *Mugil seheli* in fish farms. M. Sc. thesis, Faculty of Science, Suez Canal Univ, Egypt.

Mazzoni, T. S.; Grier, H. J. and Grassiotto, I. Q. (2010). Germline cysts and the formation of the germinal epithelium during the female gonadal morphogenesis in *Cyprinus carpio* (Teleostei: Ostariophysi: Cypriniformes). Anat. Rec., 293(9): 1581-1606.

Mercy, T. V. A.; Malika, V. and Sajan, S. (2013). Reproductive biology of *Puntius denisonii* (Day 1865): An endemic ornamental cyprinid of the Western Ghats of India. Ind. J. Fish., 60(2): 73-78.

Merson, R. R.; Casey, C. S.; Martinez, C.; Soffientino, B. and Chandlee, M. (2000). Oocyte development in summer flounder: Seasonal changes and steroid correlates. J. Fish. Biol., 57(1): 182-196.

Mourente, G.; Megina, G. and Diaz-Salvago, E. (2002). Lipids in female northern bluefin tuna (*Thunnus thynnus* L.) during sexual maturation. J. Fish Physiol. Biochem., 24: 351-363.

Nassar, A. F. A. (1993). Studies on the Biology and Reproduction of *Siganus canaliculatus*. M. Sc. thesis, Faculty of Science, zagazig Univ., Egypt.

Nayyar, R. P. (1964). The yolk nucleus of fish oocytes. Quart. J. Micros. Sci., 105: 353-356.

Rahemo, Z. I. F. and Al-Shatter, N. M. S. (2012). Observations on reproductive organs and tissues of two fresh-water cyprinid fishes, *Barbus luteus* and *Varicorhinus trutta*. J. Med. Med. Sci., 3(12): 764-773.

Ramadan, A. A.; Ezzat, A. A.; Khadre, S. E. M.; Meguid, N. A. and El-Aziz, S. H. (1987). Seasonal histological changes in the ovary of *Sparus aurata*, a hermaphrodite teleost marine fish (family: Sparidae) Folia Morphol., 35(3): 251-264.

Ravaglia, M. A. and Maggese, M. C. (2002). Oogenesis in the swamp eel, *Synbranchus marmoratus* (Bloch, 1795) (Teleostei; Synbranchidae). Ovarian anatomy, stages of oocyte development and micropyle structure. Biocell, 26(3): 325-337.

Reynolds, E. S. (1963). The use of lead citrate at high pH as an electron opaque stain in electron microscopy. J. Cell Biol., 17: 208-212.

Rizkalla, W. (1970). Studies on the gonads of the Nile Teleost fish, *Clarias lazera* C. and V., with special reference to their endocrine tissues. Acta Vet. Acad. Sci., Hung., 20: 1-12.

Rizkalla, W. and Yoakim, E. G. (1977). Studies on the ovary of the Nile catfish, *Synodontis schall* (Bloch-Schneider). III. Pre-ovulatory and post-ovulatory corpora lutea. Proc. Zool. Soc. A.R.E., 5: 239-244.

Salem, S. A. and Mohammed, S. Z. (1982). Studies on *Mugil seheli* and *Mugil capito* in Lake Timsah. I. Age and growth. Bull. Inst. Oceanog. Fish. A.R.E., 8 (1): 29-48.

Sathyanesan, A. G. (1961). Spawning periodicities as revealed by the seasonal histological changes of the gonads in *Barbus stigma* (Cuv. & Val.). Proc. Zool. Soc., 14: 15-25.

Sathyanesan, A. G. (1962). The ovarian cycle in the catfish, *Mystus seenghala* (Sykes). Proc. Natl. Inst. Sci. Ind., 28 (6): 497-506.

Selman, K. and Wallace, R. A. (1983). Oogenesis in *Fundulus heteroclitus*. III. Vitellogenesis. J. Exp. Zool., 226: 441-457.

Shakhsheir, E. (1970). Studies on some endocrine glands of a Nile teleost, *Chrysichthys auratus*, M. Sc. thesis, Faculty of Science. Ain Shams Univ., Egypt.

Shelton, W. L. (1964). The threadfin shad, *Dorosoma petenense* (Gunther): oogenesis, seasonal ovarian changes and observations on life history. M. Sc. thesis, Oklahoma State Univ., (Mimeo.).

Üçüncü, S. İ. and Çakici, Ö. (2009). Atresia and apoptosis in preovulatory follicles in the ovary of *Danio rerio* (zebrafish). J. Fish. Aquat. Sci., 9: 215-221.

Uribe, M. C.; Harry, J.; Grier, H. J. and Parenti, L. R. (2012). Ovarian structure and oogenesis of the oviparous goodeids, *Crenichthys baileyi* and *Empetrichthys latos*, (Teleostei, Cyprinodontiformes). J. Morphol., 273 (4): 371-387.

Yamamoto, K. (1963). Electron microscopy of fish development. II. Oocyte-follicle cell relationship and formation of chorion in *Oryzias latipes*. J. Fac. Sci. Univ., Tokyo, 10:123-127.

Zaki, M. I. and El-Gharabawy, M. M. (1991). Histological characters of ovaries of *Mugil capito* Egypt. J. Appl. Sci., 6(6): 13-23.

EXPLANATION OF FIGURES

Fig. 1: photographs of dissected adult females *L. carinata*, showing the morphological features of the ovaries during the different reproductive seasons; A: early post-spawning, B: late pos-spawning, C: pre-spawning and D: spawning seasons.

Fig. 2: Photomicrograph of a T.S. of the ovary of *L. carinata* in the pre-spawning season, showing the oocytes, atretic follicles, ovigerous lamellae, ovarian lumen and ovarian wall. (HX & E stain)

Fig. 3: Photomicrograph of a T.S. of the ovary of *L. carinata* in the early post-spawning season, showing the ovarian wall, peritoneal layer, tunica albuginea, longitudinal and circular muscle layers. It also shows the ovigerous lamellae, oogonia and chromatin-nucleolar oocytes. (HX & E stain)

Fig. 4: Photomicrograph of a T.S. of the ovary of *L. carinata* in the spawning season, showing the tunica albuginea. (HX & E stain)

Fig. 5: Photomicrograph of a T.S. of the ovary of *L. carinata* in the late post-spawning season, showing the oogonia, early peri-nucleolar oocytes, nuclear membrane, nuclei, nucleoli, ooplasm and vacuoles. (Toluidine blue stain)

Fig. 6: Electron micrograph of the oogonium stage of *L. carinata*, showing the nucleus, nucleolus, ooplasm, endoplasmic reticulum, ribosomes and mitochondria.

Fig. 7: Photomicrograph of a T.S. of the ovary of *L. carinata* in the spawning season, showing the chromatin-nucleolar oocyte, ooplasm, nucleus and nucleolus. (HX & E stain)

Fig. 8: Electron micrograph of the chromatin-nucleolar oocyte stage of *L. carinata*, showing the nucleus, nucleoli, nuclear membrane, ooplasm, ribosomes, mitochondria and prefollicular cell with its nucleus and chromatin patches.

Fig. 9: Electron micrograph of the chromatin-nucleolar oocyte stage of *L. carinata*, showing the oolemma of the chromatin-nucleolar oocyte, the cell membranes of the prefollicular cells and the intercellular space.

Fig. 10: Photomicrograph of a T.S. of the ovary of *L. carinata* in the pre-spawning season, showing the early peri-nucleolar oocyte, nucleus and yolk nucleus. (HX & E)

Fig. 11: Electron micrograph of the early peri-nucleolar oocyte stage of *L. carinata*, showing the ooplasm, Golgi apparatus, ribosomes, oolemma, microvilli, intercellular space and folliclar cell.

Fig. 12: Electron micrograph of the early peri-nucleolar oocyte stage of *L. carinata*, showing the nucleus, nucleoli, nuclear membrane, nuclear pore, ooplasm, granular materials and mitochondria.

Fig. 13: Photomicrograph of a T.S. of the ovary of *L. carinata* in the pre-spawning season, showing the early peri-nucleolar oocyte, oocyte wall, follicular layer, thecal layer, follicular cells, thecal cells and their nuclei. (HX & E stain)

Fig. 14: Electron micrograph of the early peri-nucleolar oocyte of *L. carinata*, showing the follicular layer, basal lamina, thecal layer, follicular cells, thecal cells, with their nuclei, chromatin patches, ribosomes and endoplasmic reticula.

Fig. 15: Electron micrograph of the early and late peri-nucleolar oocyte stages of *L. carinata*, showing the ooplasm, oolemma, intercellular space, microvilli and follicle cells.

Fig. 16: Photomicrograph of a T.S. of the ovary of *L. carinata* in the pre-spawning season, showing the late peri-nucleolar oocyte, nucleus, nucleoli and nuclear membrane. (HX & E stain)

Fig. 17: Photomicrograph of a T.S. of the ovary of *L. carinata* in the pre-spawning season, showing the early peri-nucleolar oocyte, late peri-nucleolar oocyte, vacuolated oocyte, ooplasm, yolk nucleus and vacuoles. (HX & E stain)

Fig. 18: Electron micrograph of the late peri-nucleolar oocyte stage of *L. carinata*, showing the nucleus, nucleoli, ooplasm and yolk nucleus.

Fig. 19: Electron micrograph of the late peri-nucleolar oocyte stage of *L. carinata*, showing the oocyte wall, zona radiata, microvilli, pore canals, follicular layer, basal lamina, thecal layer, follicular cell, with a nucleus, chromatin patches, nuclear membrane, endoplasmic reticulum, mitochondria and ribosomes, and the thecal cell, with the nucleus and collagenous fibers.

Fig. 20: Photomicrograph of a T.S. of the ovary of *L. carinata* in the pre-spawning season, showing the late peri-nucleolar oocyte, oocyte wall, zona radiata, follicular layer and thecal layer. (HX & E stain)

Fig. 21: Photomicrograph of a T.S. of the ovary of *L. carinata* in the spawning season, showing the vacuolated oocyte, nucleus, ooplasm and vacuoles. (HX & E stain)

Fig. 22: Photomicrograph of a T.S. of the ovary of *L. carinata* in the spawning season, showing the vacuolated oocyte, nucleus, nucleoli in outpocketings and nuclear membrane. (HX & E stain)

Fig. 23: Electron micrograph of the vacuolated oocyte stage of *L. carinata*, showing the nucleus, nuclear membrane, nucleoli and lipid droplets.

Fig. 24: Electron micrograph of the vacuolated oocyte stage of *L. carinata*, showing the lipid droplets, mitochondria and vacuoles.

Fig. 25: Photomicrograph of a T.S. of the ovary of *L. carinata* in the spawning season, showing the vacuolated oocyte, zona radiata, follicular layer and thecal layer. (HX & E stain)

Fig. 26: Electron micrograph of the vacuolated oocyte stage of *L. carinata*, showing the zona radiata, pore canals, oocyte wall, follicular layer, basal lamina, thecal layer and follicular cell.

Fig. 27: Electron micrograph of the vacuolated oocyte stage of *L. carinata*, showing the zona radiata, pore canals, oocyte wall, follicular layer, basal lamina, thecal layer and thecal cell.

Fig. 28: Photomicrograph of a T.S. of the ovary of *L. carinata* in the spawning season, showing the early yolk globular oocyte, nucleus, nucleoli, ooplasm and yolk granules. (HX & E stain)

Fig. 29: Photomicrograph of a T.S. of the ovary of *L. carinata* in the spawning season, showing the early yolk globular oocyte, nucleus, ooplasm, yolk granules and vacuoles. (HX & E stain)

Fig. 30: Photomicrograph of a T.S. of the ovary of *L. carinata* in the spawning season, showing the early yolk globular oocyte, yolk granules, ooplasm, vacuoles, zona radiata, follicular layer and thecal layer. (HX & E stain)

Fig. 31: Electron micrograph of the early yolk globular oocyte stage of *L. carinata*, showing the ooplasm, yolk granules, lipid droplets, vacuoles.

Fig. 32: Electron micrograph of the early yolk globular oocyte stage of *L. carinata*, showing the yolk granules accumulation from the outside (white arrowheads), yolk granule, ooplasm, zona radiata and pore canals.

Fig. 33: Electron micrograph of the early yolk globular oocyte stage of *L. carinata*, showing the oocyte wall, zona radiata, zona radiata interna, zona radiata externa, pore canals and microvilli, follicular layer, basal lamina, thecal layer, follicular cell and thecal cell.

Fig. 34: Photomicrograph of a T.S. of the ovary of *L. carinata* in the spawning season, showing the late yolk globular oocytes. (HX & E stain)

Fig. 35: Photomicrograph of a T.S. of the ovary of *L. carinata* in the spawning season, showing the late yolk globular oocyte, yolk globules, vacuoles and nucleus. (HX & E stain)

Fig. 36: Photomicrograph of a T.S. of the ovary of *L. carinata* in the spawning season, showing the late yolk globular oocyte, oocyte wall, zona radiata, follicular layer and thecal layer. (HX & E stain)

Fig. 37: Electron micrograph of the late yolk globular oocyte stage of *L. carinata*, showing the oocyte wall, zona radiata, zona radiata interna, zona radiata externa, pore canals, follicular layer, basal lamina and thecal layer.

Fig. 38: Electron micrograph of the late yolk globular oocyte stage of *L. carinata*, showing the oocyte wall, zona radiata, zona radiata interna, zona radiata externa, pore canals, follicular layer, basal lamina, thecal layer, follicular cell and thecal cell with their nuclei.

Fig. 39: Photomicrograph of a T.S. of the ovary of *L. carinata* in the early post-spawning season, showing the post-ovulatory structure. (HX & E stain)

Fig. 40: Photomicrograph of a T.S. of the ovary of *L. carinata* in the late post-spawning season, showing the atretic follicle, zona radiata, follicular layer, follicular cells and liquefied yolk. (HX & E stain)

Fig. 41: Photomicrograph of a T.S. of the ovary of *L. carinata* in the late post-spawning season, showing the atretic follicle, zona radiata, follicular layer, follicular cells and liquefied yolk. (Toluidine blue stain)

Fig. 42: Photomicrograph of a T.S. of the ovary of *L. carinata* in the late post-spawning season, showing the atretic follicle, zona radiata, follicular cells and liquefied yolk. (Toluidine blue stain).

LIST OF ABBREVIATION

|	
At.fc	Atretic follicles.
Bs.lam	Basal lamina.
Ce.mm	Cell membrane.
Ch.nu.oo	Chromatin-nucleolar oocytes.
Ch.pat	Chromatin patches.
Cr.ms.l	Circular muscle layer.
En.r	Endoplasmic reticulum.
Er.pe.nu.oo	Early peri-nucleolar oocyte.
Er.yo.gl.oo	Early yolk globular oocyte.
Fc.ce	Follicular cell.
Fc.l	Follicular layer.
G.ap	Golgi apparatus.
Gr.ma	Granular material.
Ice.spa	Intercellular space.
La. pe.nu.oo	Late peri-nucleolar oocyte.
La.yo.gl.oo	Late yolk globular oocyte.
Li.dr	Lipid droplets.
Lo.ms.l	Longitudinal muscle layer.
Lq.yo	Liquefied yolk.
M	Mitochondria.
Mv	Microvilli.
N	Nucleus.
N.mm	Nuclear membrane.
N.por	Nuclear pore.
Nu	Nucleolus.
Og.lm	Ovigerous lamellae.
Ogn	Oogonium.
Olm	Oolemma.
Oo	Oocyte.
Oo.w	Oocyte wall.
Op	Ooplasm.
Out	Outpocketing.
Ov	Ovary.
Ov.lu	Ovarian lumen.
Ov.w	Ovarian wall.
Pfc.ce	Prefollicular cell.
Por.ca	Pore canal.
Pr.l	Peritoneal layer.
Ps.ovu.st	Post ovulatory structures.
Ri	Ribosomes.
Th.ce	Thecal cell.
Th.l	Thecal layer.
Tu.al	Tunica albuginea.
V	Vacuoles.
V.oo	Vacuolated oocyte.
Yo.gl	Yolk globules.
Yo.gr	Yolk granules.
Yo.n	Yolk nucleus.
Zn.ra	Zona radiata.
Zn.ra.e	Zona radiata externa.
Zn.ra.i	Zona radiata interna.
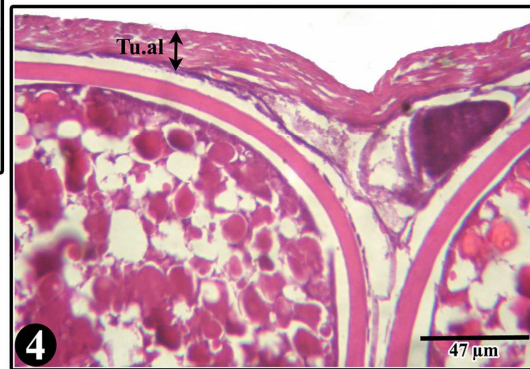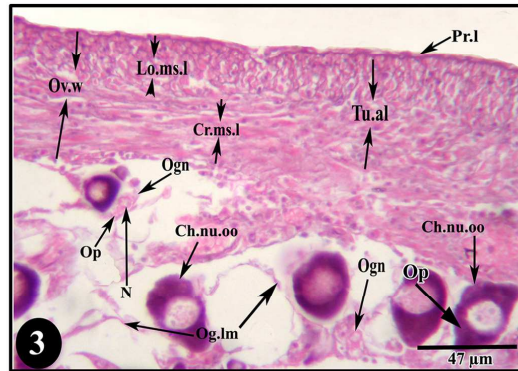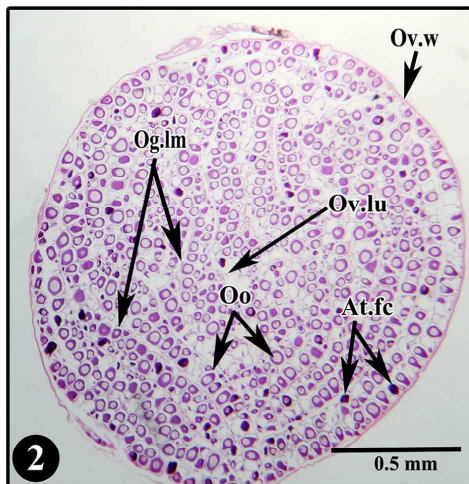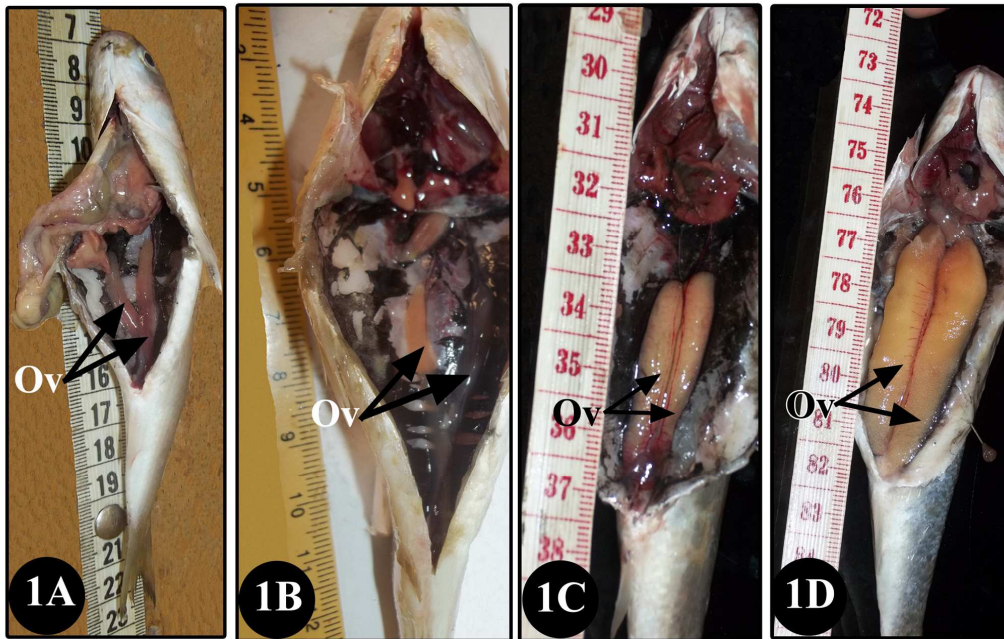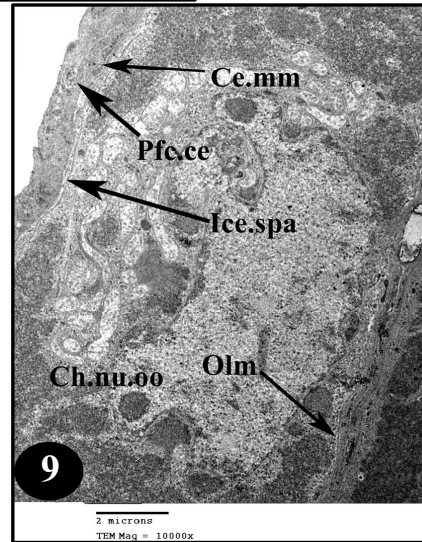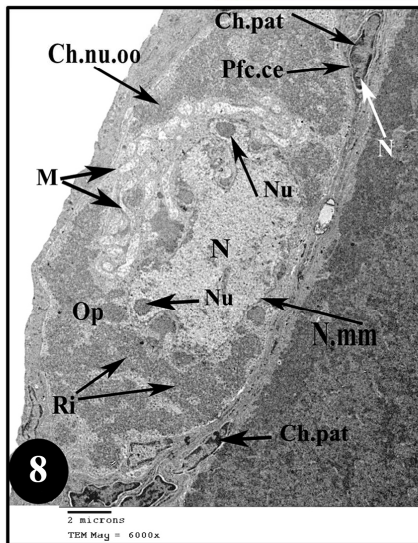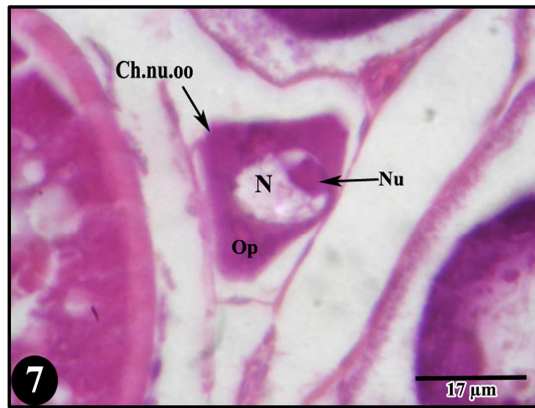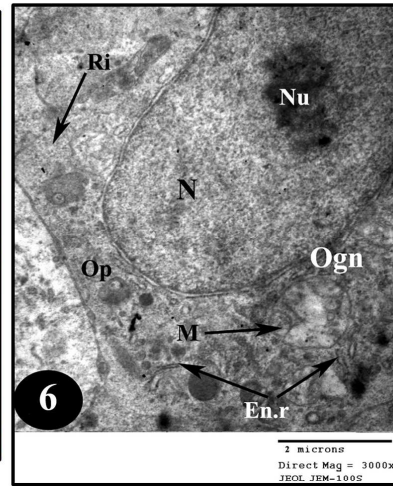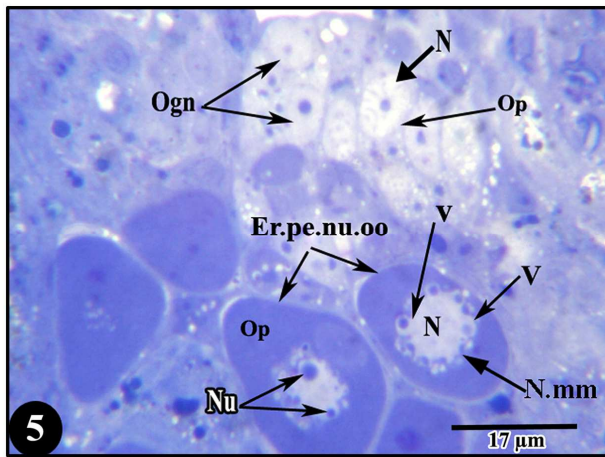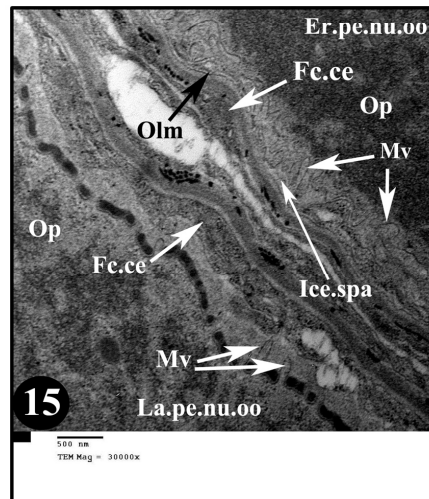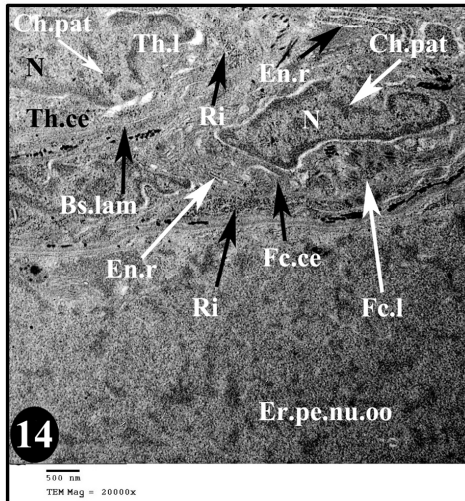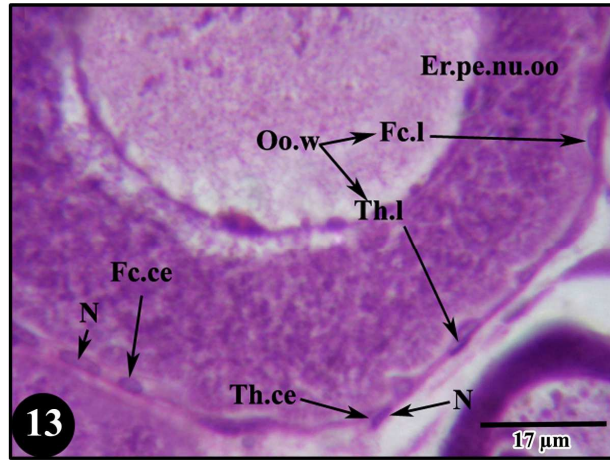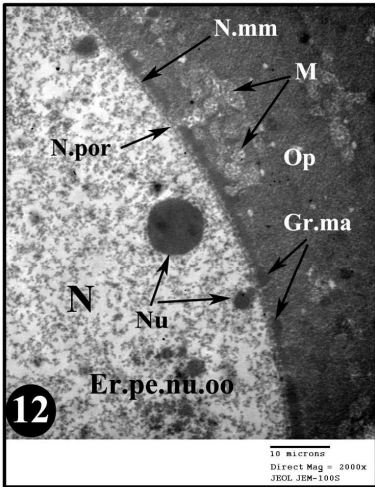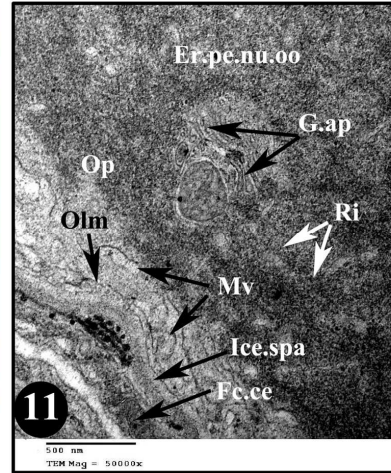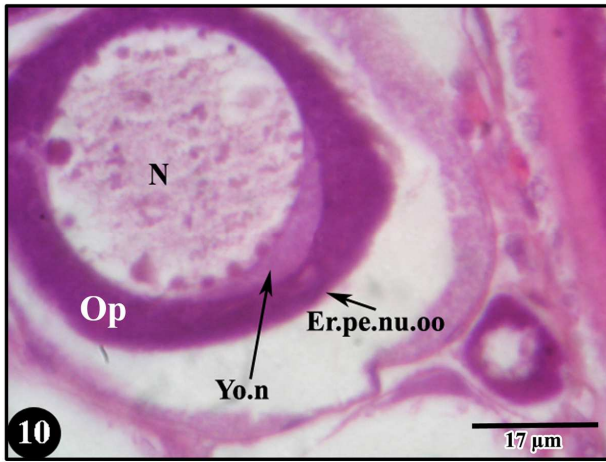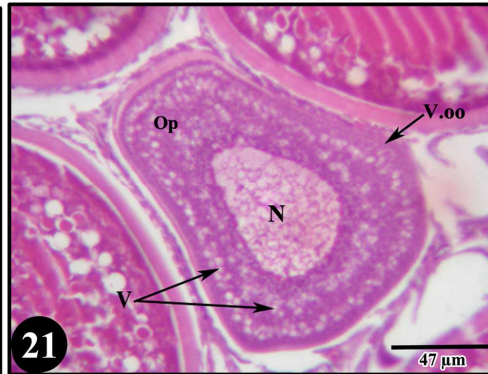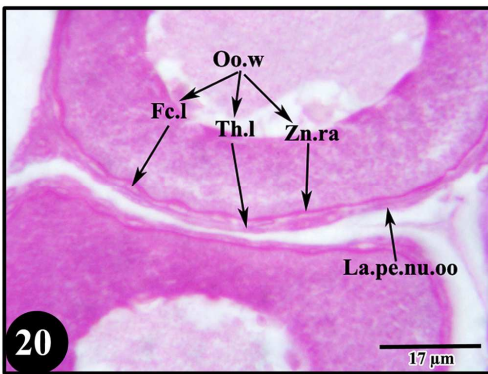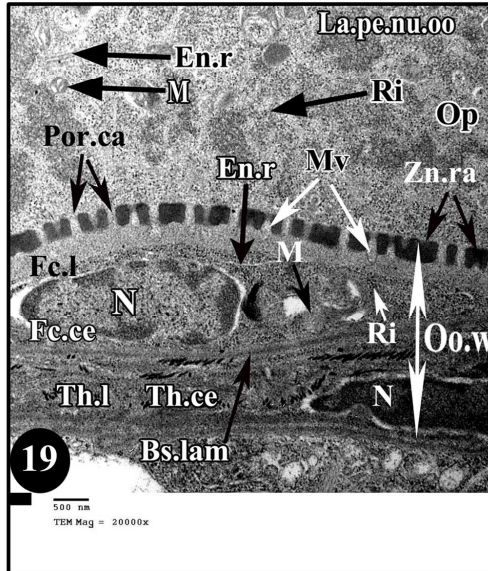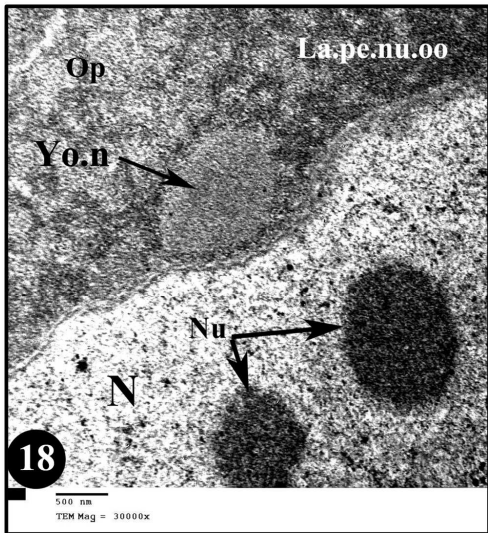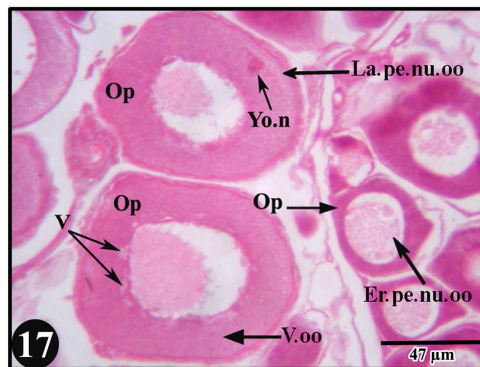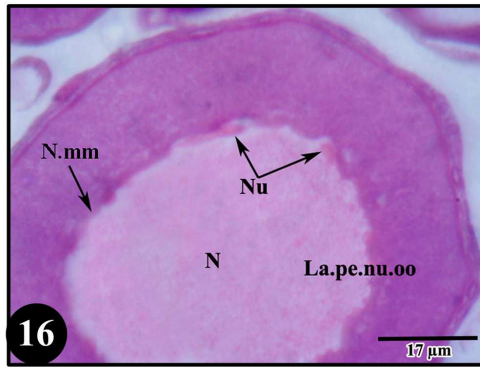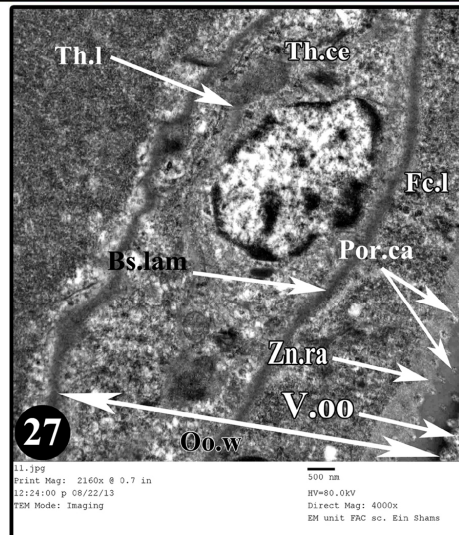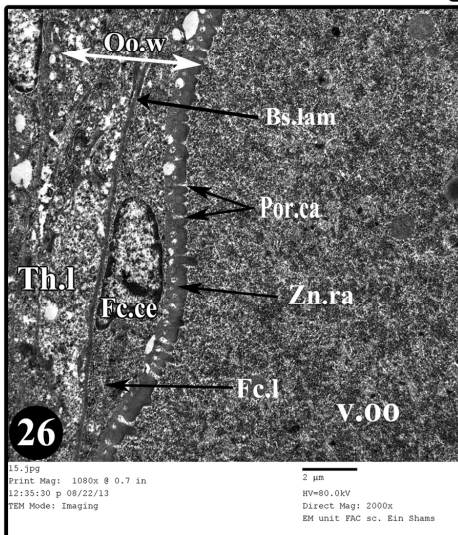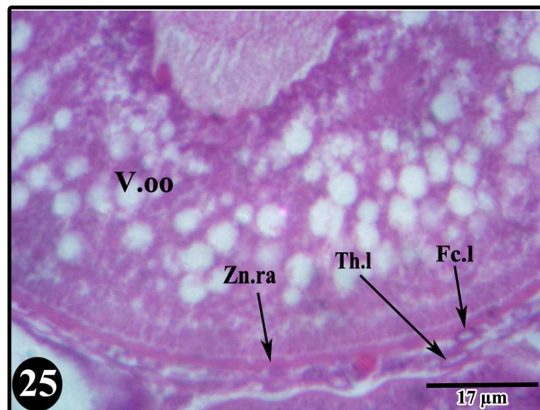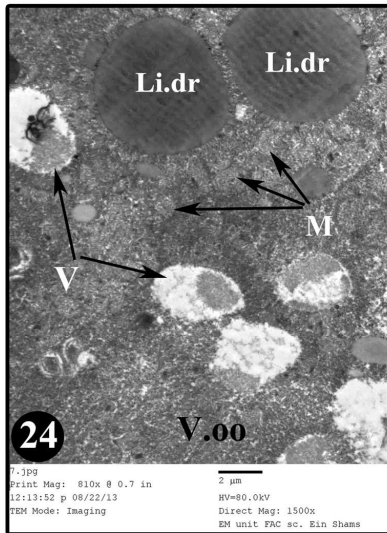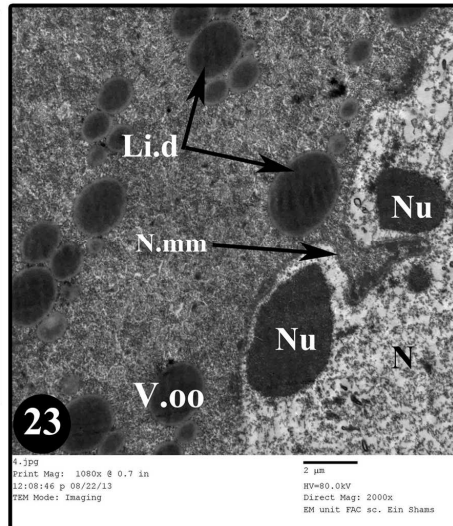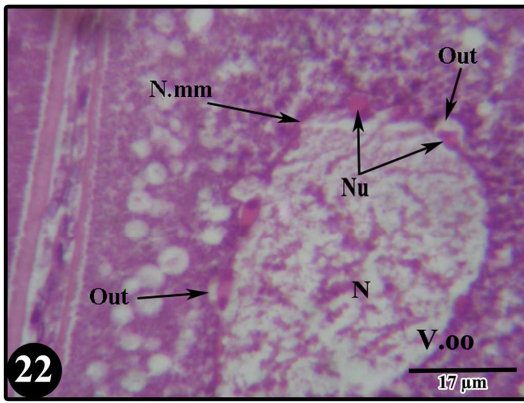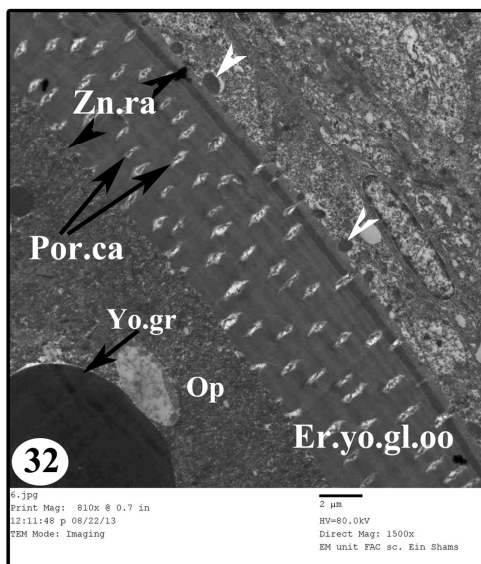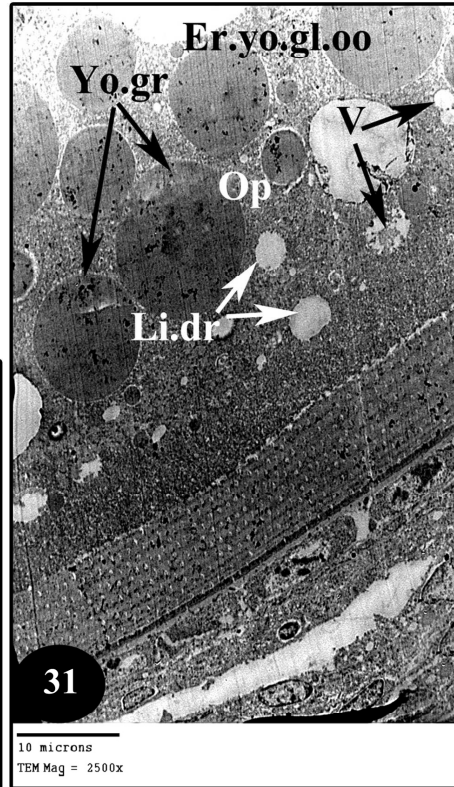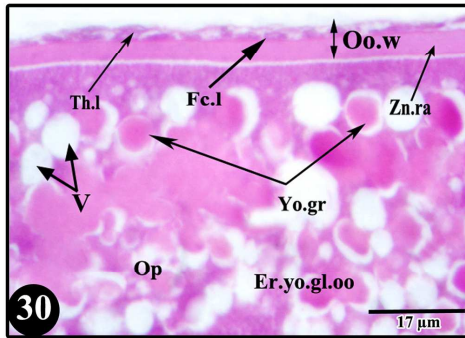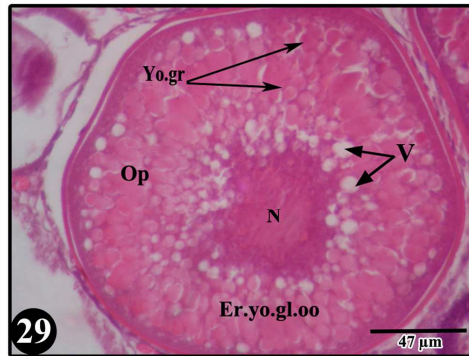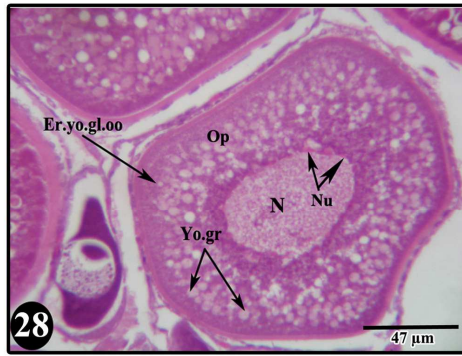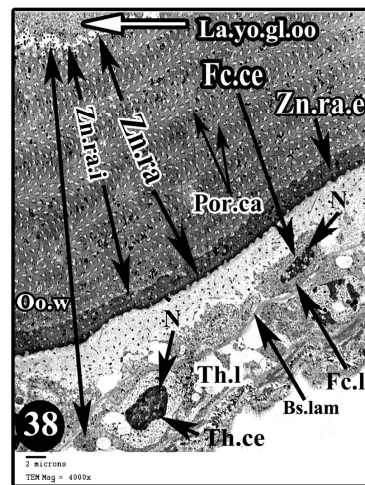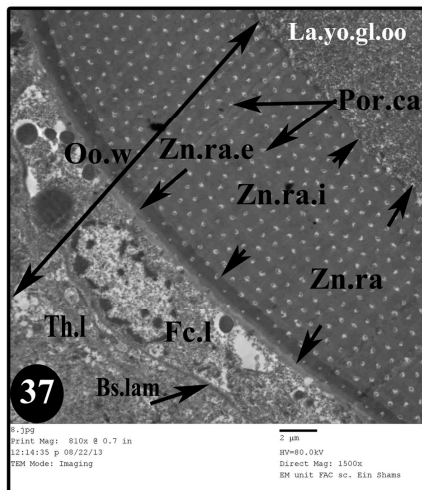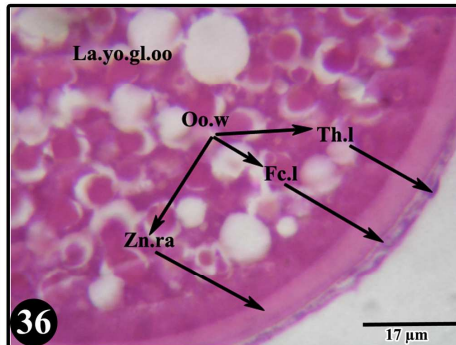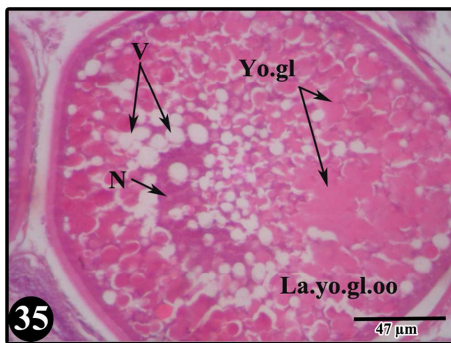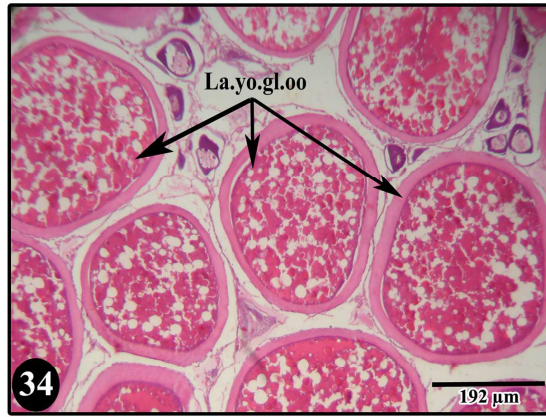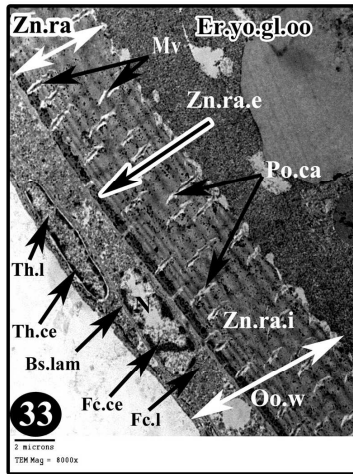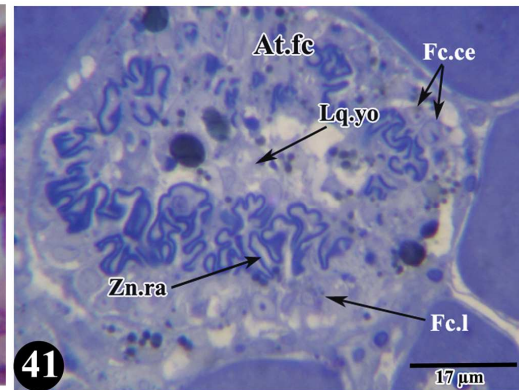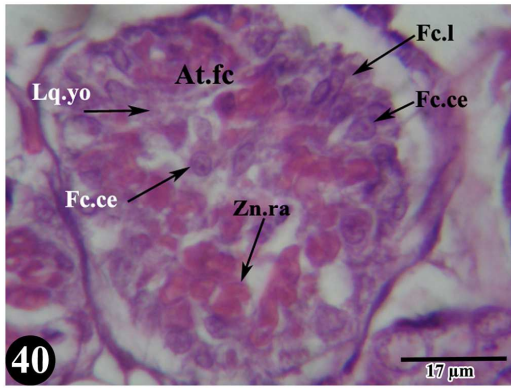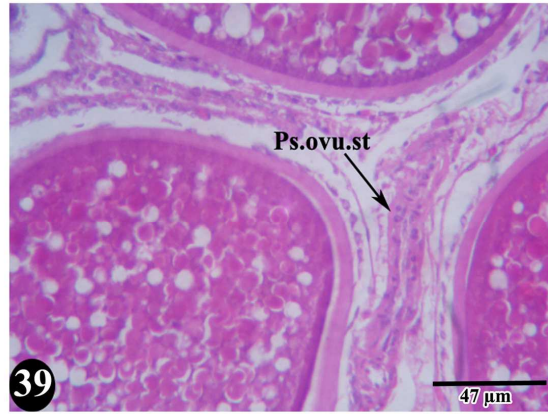
ARABIC SUMMARY

دراسات مورفولوجية ونسيجية وتركيبية دقيقة على مبايض أسماك السهلية من خليج السويس و ارتباطها بدورتها التناسلية

فوزية عاشور عبد الغفار عبد الرحمن[1] و حمزة احمد الشبكة[1] و وليم رزق الله[1] وعزة عبد الحميد الجانينى[2] و مزاية السيد أبو مسلم[1]

١- قسم علم الحيوان- كلية العلوم- جامعة عين شمس- القاهرة.
٢- معهد علوم البحار والمصايد- فرع السويس- السويس.

تعتبر أسماك السهلية من أسماك العائلة البورية ذات الأهمية الاقتصادية، ولذلك كانت دراسة دورتها التناسلية ذات أهمية قصوى للمساهمة فى إدارة مزارعها السمكية. ولقد إهتم البحث الحالى بدراسة التركيب المورفولوجي و النسيجى و النسيجى الدقيق لمبايض سمكة السهلية و ارتباطه بدورتها التناسلية فى خليج السويس.

ولقد أظهرت الدراسة المورفولوجية أن المبيض فى سمكة السهلية يمر بأربعة مواسم وهى موسم مابعد التبويض المبكر وموسم مابعد التبويض المتأخر و موسم ماقبل التبويض و موسم التبويض. كما وجد ان موسم التبويض يمتد من نهاية شهر سبتمبر و حتى نهاية شهر ديسمبر.

كما أوضح التركيب النسيجى و التركيب النسيجى الدقيق لمبايض أسماك السهلية انه يحتوى على بويضات فى مراحل مختلفة من النمو، والتى أمكن تقسيمها إلى سبعة مراحل مختلفة، بالإضافة الى تركيبات ما بعد التبويض و كذلك البويضات المتحللة.